Electronic Supplemental Information

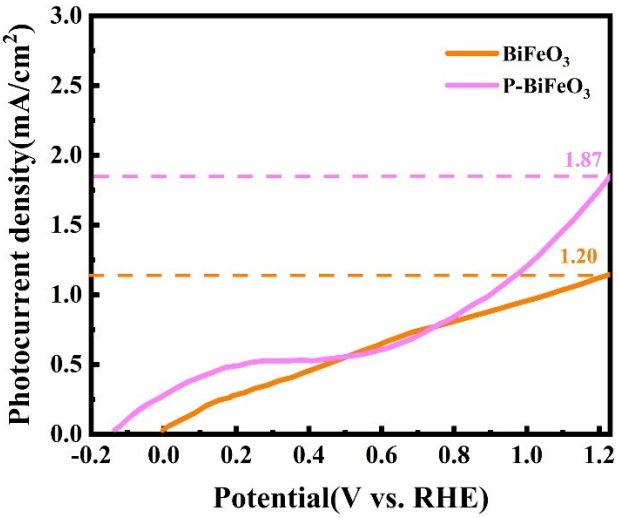

Fig. S1 LSV curves of $BiFeO_3$, P-$BiFeO_3$ photoanodes measured in 0.2 M Na_2SO_4 electrolyte solution with the addition of 0.1 M Na_2SO_3

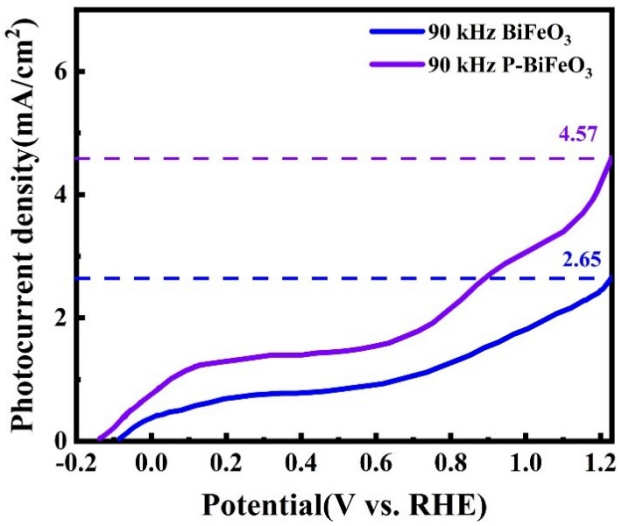

Fig. S2 LSV curves of $BiFeO_3$, P-$BiFeO_3$ photoanodes measured in 0.2 M Na_2SO_4 electrolyte solution with the addition of 0.1 M Na_2SO_3 under 90 kHz ultrasonic vibration

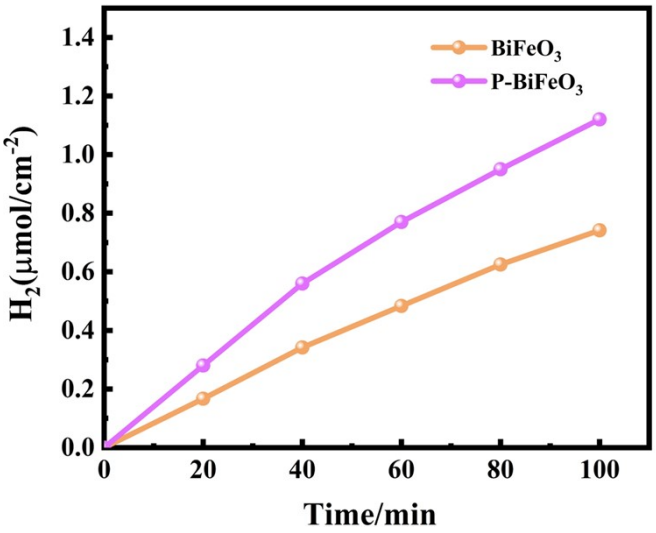

Fig. S3 Hydrogen evolution curve measured under AM 1.5G continuous illumination

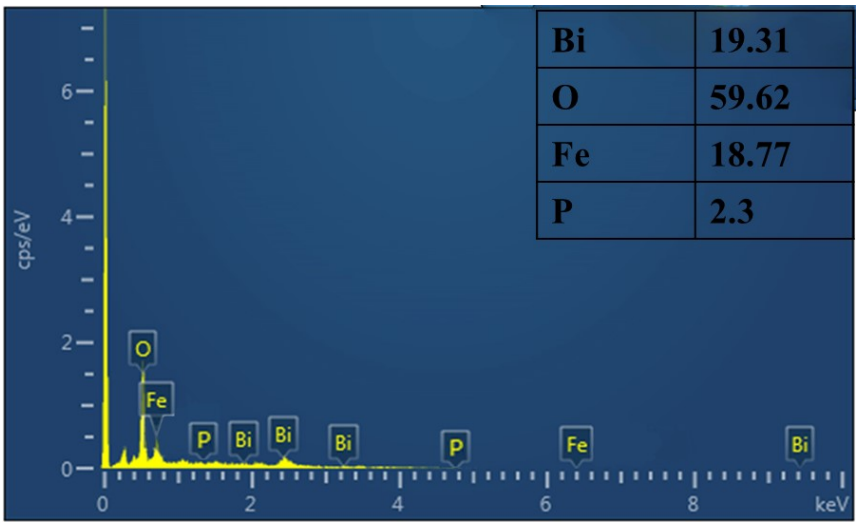

Fig. S4 EDS elemental mapping diagram of P-$BiFeO_3$

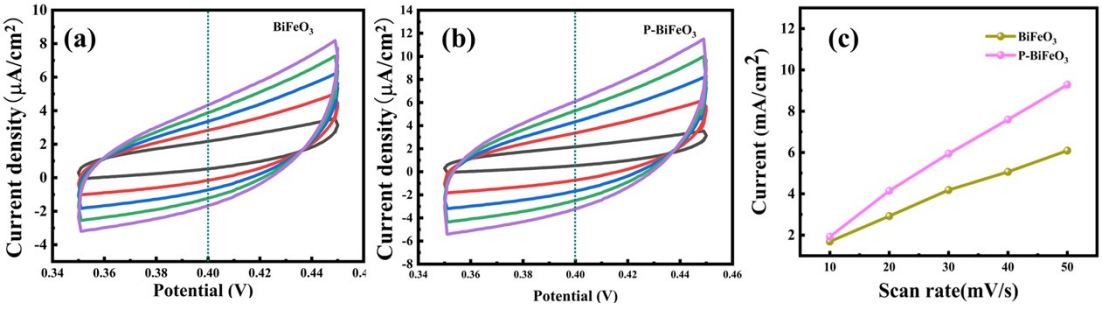

Fig. S5 CV of $BiFeO_3$ (a) and P-$BiFeO_3$(b) photoanodes performed at different scan rates; Charging current density differences of $BiFeO_3$ and P-$BiFeO_3$ (c) photoanodes plotted against scan rates

Tab. S1 The flat band potential (V_{FB}) and carrier density (N_d) of $BiFeO_3$ and P-$BiFeO_3$ photoanodes with different conditions

Samples	**V_{FB} (V vs RHE)**	**N_d (cm^{-3})**
$BiFeO_3$	0.57	3.5×10^{13}
P-$BiFeO_3$	0.55	4.2×10^{13}
$BiFeO_3$ under 90 kHz ultrasonic vibration	0.47	3.7×10^{14}
P-$BiFeO_3$ under 90 kHz ultrasonic vibration	0.43	1.9×10^{15}

Tab. S2 The fitted parameters extracted from Nyquist plots of $BiFeO_3$ and P-$BiFeO_3$ photoanodes with different conditions

Samples	**R_1 (Ω cm^2)**	**R_2 (Ω cm^2)**	**W_1(Ω cm^2)**	**CPE(F/cm^2)**
$BiFeO_3$	30.24	2275	0.36970	0.89574
P-$BiFeO_3$	28.26	2232	0.59625	0.87823
$BiFeO_3$ under 90 kHz ultrasonic vibration	17.76	478	0.33245	0.81254
P-$BiFeO_3$ under 90 kHz ultrasonic vibration	14.12	402	0.21351	0.89325